JOURNAL OF INFORMATION SCIENCE AND ENGINEERING 26, 1049-1071 (2010)

Robust Image Watermarking Using Adaptive Structure Based Wavelet Tree Quantization

GIN-DER WU AND PANG-HSUAN HUANG
Department of Electrical Engineering
National Chi Nan University
Puli, 545 Taiwan

This work presents a novel robust wavelet-tree-based watermarking method based on structure-based quantization. Wavelet-trees are arranged into super-trees. The watermark bits are then embedded into the super-trees by using the proposed structure-based quantization method. Next, the super-trees are quantized into a significant structure according to these bits. The quantized super-tree has a stronger statistical characteristic than the unquantized super-tree. Based on this characteristic, the watermark bits could be extracted robustly after an image distortion attack. Finally, an adaptive method is developed to raise the PSNR value. Compared with Wang *et al.* [17] method, the proposed adaptive method increases PSNR about 5.83dB. The proposed method also has a higher maximum number of watermark bits than other methods, thus increasing the capacity for embedding. Besides, its computation load is low. Experimental results demonstrate that the proposed watermarking method using adaptive structure-based wavelet-tree quantization performs well in JPEG compression, filtering (Gaussian filter, median filter and sharpen) and geometric attacks (pixel shifting and rotation). In addition, it is very robust against multiple watermark attacks.

Keywords: wavelet-tree, structure-based quantization, super-trees, statistical characteristic, PSNR

1. INTRODUCTION

Owing to the accelerated development of digital signal processing, most multimedia data are stored digitally. Since the Internet enables users to obtain data easily, they can obtain unsecured personal data of others. Hence, users can modify data for which they do not own the copyright. To solve this problem, a mechanism is required to protect copyrighted data. Hence, data protection has become a significant topic in recent years. This work presents a method for image copyright protection. Digital watermarking is a conventional means of protecting image ownership, in which copyright owners embed copyright messages, such as serial numbers, badges or signatures, into host images.

Many digital watermarking methods have been proposed. Watermarking techniques are typically categorized as visible [1-3] or invisible [4-22] ones. Invisible watermarking methods are further categorized as the spatial domain [4-6] and transform domain [7-19]. In DCT (Discrete Cosine Transform) based methods [7-9], the host image is divided into several subblocks, which are transformed by using DCT. The watermark message is applied into the frequency coefficients of these subblocks. Compared with direct modifying pixels, modifying the frequency coefficients reduces the distortion of the host image, and saves the quality of watermarked images. Moreover, the frequency domain has a high

Received May 27, 2008; revised October 24, 2008; accepted February 27, 2009.
Communicated by H. Y. Mark Liao.

capacity to embed watermark bits.

DWT (Discrete Wavelet Transform) has recently become the most popular watermarking technique. Several DWT methods have been proposed [10-19]. In DWT based watermarking, the host image is converted into several subbands by using multiresolution decomposition. To achieve different proposals, the watermark bits are embedded into different selected subbands. To balance the quality and robustness, the watermark is typically embedded into middle subbands. Some methods [11, 12] embed the watermark by using the relationship between coefficients in different subbands. Media-data dependent quantization has also been developed to embed watermarks [13]. It not only embeds watermark, but also locates the part of an image that has been tampered with. In [14], the watermark is not embedded into host image directly. It is applied by special transform first. This approach has strong robustness to against data compression systems such as JPEG. Multiresolution wavelet decomposition [15-17] obtains a significant tree structure, which is then adopted to embed the watermark.

Watermark is embedded by using wavelet-tree quantization in [17]. The host image is transformed into the DWT domain, and pairs of wavelet-trees are combined into so-called super-trees. Each bit is then embedded in a pair of super-trees, which is spread into the bitplane and quantized according to the bit state. A quantization index is then generated to determine how much information should be quantized. The quantization index is counted from right to left, and down to up, in the bitplane. The bits below the selected quantization index after quantization are discarded. To extract the watermark, this pair of super-trees is passed through the maximum likelihood detector. It determines the bit state by processing the bitplane of these two super-trees and deciding which one has been quantized previously.

The digital signature is another different proposition to protect the copyright [18, 19]. The content information or the feature of original images is extracted and stored. It could be used to verify whether the host image has been modified. The false alarm (false positive) and missed detection (false negative) probabilities must be considered as well. The false alarm probability is the probability of a false watermark being detected as true. A missed detection means that a watermark exists, but is not extracted by the watermark detector. These issues concern the reliability of watermarking [11, 17, 19].

In this paper, we present a novel watermarking technique by quantizing the wavelet-tree into a significant structure. It can balance the quality and the robustness without substantial computational load. Then, a voting system is adopted in the watermark extraction process. It is designed according to the unbalanced stability in different decomposition levels. Therefore, the robustness is further increased. Finally, an adaptive method is presented to enhance the quality of embedding. Experiments show that PSNR is highly increased by using this adaptive method. In addition, experimental results demonstrate that the proposed method can resist several attacks include JPEG compression, filtering (Gaussian filter, median filter and sharpen) and geometric attacks (pixel shifting and rotation).

2. STRUCTURE-BASED WATERMARKING

In this section, we briefly introduce the two-dimensional DWT and the super-tree. Then the novel structure-based watermark embedding and extraction methods will be proposed later.

2.1 Flowchart of Watermarking Method

Fig. 1 is the flowchart of watermarking method for the copyright protection. The block diagram of the watermark embedding flow is shown in Fig. 1 (a). The host image is transformed into wavelet domain by using DWT, and the coefficients are grouped into wavelet-trees. The watermark data W is a binary sequence of ± 1. It is generated by a one-way deterministic function [22]. Then the wavelet-trees and the binary watermark sequence are processed by watermark encoder. The encoder fuses the bits with the wavelet-trees by quantizing the wavelet-trees into a significant structure. Compared with the unquantized wavelet-tree, the quantized version has strong statistical characteristic. Therefore, the watermark could be extracted easily by this property. After watermark encoding, these quantized coefficients are applied by IDWT to produce a watermarked image.

The extraction flow is shown in Fig. 1 (b). The watermarked image is transformed into wavelet-trees. Then these wavelet-trees pass the watermark detector. This decoder will extract the watermark sequence W' and compare it with the original watermark sequence W. By calculating the normalized correlation Φ, a threshold Φ_T will be used to judge whether the extracted watermark is true or not. We say that the watermark is true to exist if the normalized correlation Φ exceeds the threshold Φ_T. However, the watermark does not exist if Φ is smaller than the threshold Φ_T.

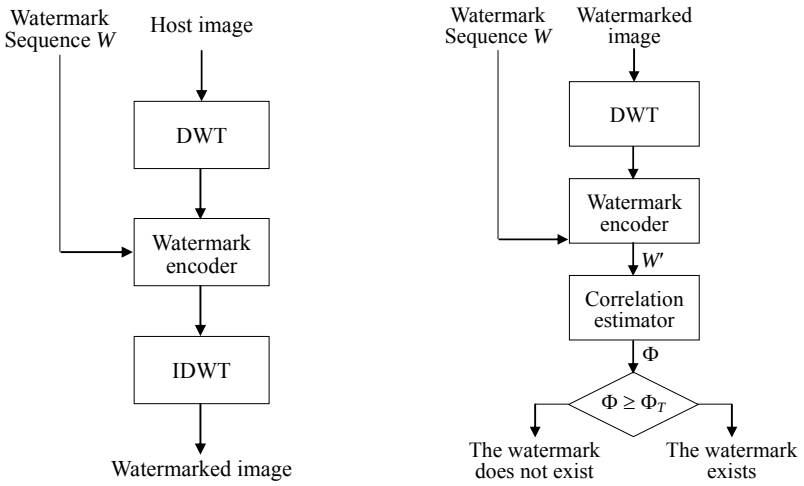

Fig. 1. (a) Block diagram of the proposed watermark embedding flow; (b) Block diagram of the proposed watermark extraction flow.

2.2 Structure-based Super-tree

In this subsection, we describe the detail of DWT and tree structure. A 512×512 image is used as an example. In Fig. 2 (a), an image is decomposed into four subbands and labeled as LL1, LH1, HL1 and HH1 (low-low, low-high, high-low and high-high frequency domain) by applying one-level DWT. To implement two-level decomposition,

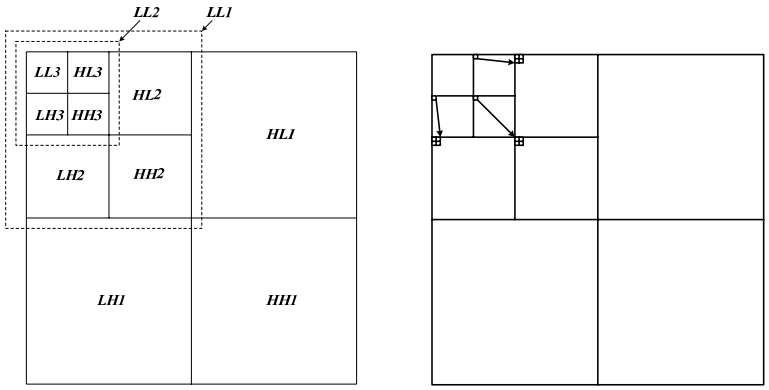

(a) (b)

Fig. 2. (a) A three-level wavelet decomposition and 10 subbands; (b) The wavelet-trees.

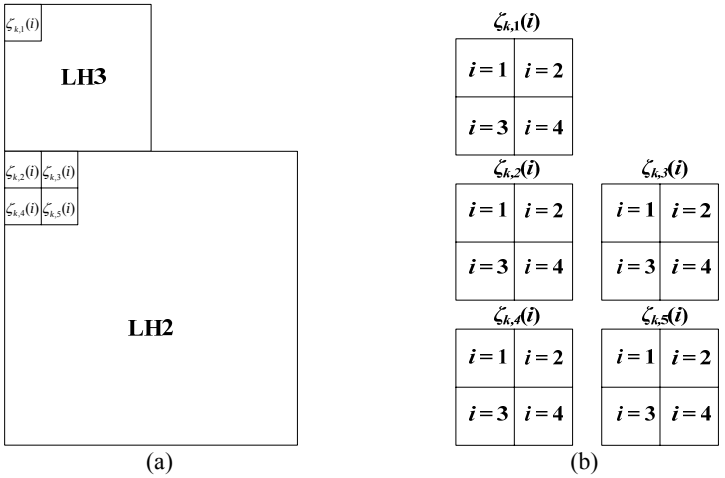

(a) (b)

Fig. 3. (a) Coefficients in a super-tree; (b) Subblocks of a super-tree.

the LL1 is selected and decomposed again. Finally, the LL2 is further decomposed, and the host image is totally decomposed into 10 subbands by three-level DWT. In Fig. 2 (b), the wavelet-tree structure is defined by the relationship between the coefficients in the same spatial location at different level. Furthermore, the host image could be reconstructed by IDWT (inverse DWT). We say the host image is perfect reconstructed if the reconstructed image is only suffered from time delay or scaling.

Since we group the coefficients of the same spatial location to be a tree, there are totally $64 \times 64 \times 3$ trees in Fig. 2 (b). We will use the coefficients in level two (LH2, HH2 and HL2) and level three (LH3, HH3 and HL3) for watermarking. Therefore, each tree has 5 coefficients. These coefficients of the same tree correspond to different frequency bands. For structure-based quantization, we arrange the trees to form a super-tree in Fig. 3 (a). Since a super-tree is composed of five 2×2 subblocks shown in Fig. 3 (b), there are totally 20 coefficients in each super-tree and denoted by

$$\zeta_{k,m}(i),\ 1 \le k \le 3072;\ 1 \le m \le 5;\ 1 \le i \le 4, \tag{1}$$

where k is the index of super-tree, m is the index of the subblock in a super-tree, and i is the index of the element in a subblock. Fig. 3 (a) shows the relationship between the coefficients in a super-tree. Since each watermark bit W_n is embedded by using one super-tree, the maximum number of watermark bits is $32 \times 32 \times 3 = 3072$.

To enhance the security of the watermark, the super-trees are passed through a non-overlapping random mapping process as follows

$$\zeta_{n,m}(i) = f(\zeta_{k,m}),\ 1 \le n \le 3072;\ 1 \le k \le 3072, \tag{2}$$

where the transfer function $f(.)$ is the random mapping process which results in a random sequence of the super-trees. Based on $f(.)$, the watermark bits are embedded into super-trees randomly. This random mapping function is dumped as a key. Only the owner has the key to access the watermark.

After random mapping, we will apply the proposed structure-based quantization to all super-trees in vertical direction. This proposed quantization bases on a 2×2 sub-block in Fig. 4. It is denoted as $\zeta_{n,m}(i)$. We calculate the average value of the "upper" two elements ($\zeta_{n,m}(1)$, $\zeta_{n,m}(2)$) and the average of the "lower" two elements ($\zeta_{n,m}(3)$, $\zeta_{n,m}(4)$) as follows

$$\begin{aligned} \sigma_{n,m}(Up) &= \frac{\zeta_{n,m}(1) + \zeta_{n,m}(2)}{2}, \\ \sigma_{n,m}(Lo) &= \frac{\zeta_{n,m}(3) + \zeta_{n,m}(4)}{2}. \end{aligned} \tag{3}$$

If we embed a bit W_n in vertical direction, $\sigma_{n,m}(Up)$ and $\sigma_{n,m}(Lo)$ will be quantized into a significant structure as $\sigma'_{n,m}(Up)$ and $\sigma'_{n,m}(Lo)$ which are given by the following equations

$$\sigma'_{n,m}(Up) > \sigma'_{n,m}(Lo), \text{ if } W_n = -1, \tag{4a}$$

$$\sigma'_{n,m}(Up) < \sigma'_{n,m}(Lo), \text{ if } W_n = 1, \tag{4b}$$

where $\sigma'_{n,m}(Up)$ and $\sigma'_{n,m}(Lo)$ are the results of quantization. While embedding bit W_n is "– 1", $\sigma'_{n,m}(Up)$ will be bigger than $\sigma'_{n,m}(Lo)$. If embedding bit W_n is "1", $\sigma'_{n,m}(Up)$ will be smaller than $\sigma'_{n,m}(Lo)$.

$\zeta_{n,m}(1)$	$\zeta_{n,m}(2)$
$\zeta_{n,m}(3)$	$\zeta_{n,m}(4)$

Fig. 4. 2×2 subblock of $\zeta_{n,m}$ for $i = 1, 2, 3, 4$.

2.3 Watermark Embedding Method

There are several methods to satisfy Eq. (4). For example, we can use the fixed proportion method. This method makes the ratio of $\sigma'_{n,m}(Up)$ and $\sigma'_{n,m}(Lo)$ to be a fixed number (*i.e*. 1/4 or 1/8). However, this fixed proportion method does not perform well to retain the quality of the watermarked image. The reason is the coefficients of the subblock will be changed hugely, and the contrast between coefficients will be decreased obviously. In order to solve the above drawback, a novel method of structure-based wavelet-tree quantization is proposed to satisfy Eq. (4). This method will not only preserve the original information of the tree precisely but also decrease the distortion. The structure of the subblock will be modified according to several conditions which are bounded by a quantization step size Δ. Fig. 5 shows the flowchart of the proposed structure-based quantization. In this figure, the value of $\zeta_{n,m}(i)$ will be quantized to satisfy Eq. (4). For clear understanding, Eqs. (5)-(8) correspond to Fig. 5. We use $Q[.]$ to denote the quantization process. The detail is described as follows

$$Q[\zeta_{n,m}(i)]\big|_{W_n=-1}^{i=1,2}=\begin{cases}\zeta_{n,m}(i)+\dfrac{\Delta}{2}, & \text{if } \sigma_{n,m}(Up)=\sigma_{n,m}(Lo).\\ \zeta_{n,m}(i), & \text{if } \sigma_{n,m}(Up)>\sigma_{n,m}(Lo) \text{ and } dif_v\ge\Delta.\\ \zeta_{n,m}(i)+\dfrac{\Delta-dif_v}{2}, & \text{if } \sigma_{n,m}(Up)>\sigma_{n,m}(Lo) \text{ and } dif_v<\Delta.\\ \zeta_{n,m}(i)+dif_v, & \text{if } \sigma_{n,m}(Lo)>\sigma_{n,m}(Up) \text{ and } dif_v\ge\Delta.\\ \zeta_{n,m}(i)+\dfrac{dif_v+\Delta}{2}, & \text{if } \sigma_{n,m}(Lo)>\sigma_{n,m}(Up) \text{ and } dif_v<\Delta.\end{cases} \quad (5)$$

$$Q[\zeta_{n,m}(i)]\big|_{W_n=-1}^{i=3,4}=\begin{cases}\zeta_{n,m}(i)-\dfrac{\Delta}{2}, & \text{if } \sigma_{n,m}(Up)=\sigma_{n,m}(Lo).\\ \zeta_{n,m}(i), & \text{if } \sigma_{n,m}(Up)>\sigma_{n,m}(Lo) \text{ and } dif_v\ge\Delta.\\ \zeta_{n,m}(i)-\dfrac{\Delta-dif_v}{2}, & \text{if } \sigma_{n,m}(Up)>\sigma_{n,m}(Lo) \text{ and } dif_v<\Delta.\\ \zeta_{n,m}(i)-dif_v, & \text{if } \sigma_{n,m}(Lo)>\sigma_{n,m}(Up) \text{ and } dif_v\ge\Delta.\\ \zeta_{n,m}(i)-\dfrac{dif_v+\Delta}{2}, & \text{if } \sigma_{n,m}(Lo)>\sigma_{n,m}(Up) \text{ and } dif_v<\Delta.\end{cases} \quad (6)$$

$$Q[\zeta_{n,m}(i)]\big|_{W_n=1}^{i=1,2}=\begin{cases}\zeta_{n,m}(i)-\dfrac{\Delta}{2}, & \text{if } \sigma_{n,m}(Up)=\sigma_{n,m}(Lo).\\ \zeta_{n,m}(i), & \text{if } \sigma_{n,m}(Lo)>\sigma_{n,m}(Up) \text{ and } dif_v\ge\Delta.\\ \zeta_{n,m}(i)-\dfrac{\Delta-dif_v}{2}, & \text{if } \sigma_{n,m}(Lo)>\sigma_{n,m}(Up) \text{ and } dif_v<\Delta.\\ \zeta_{n,m}(i)-dif_v, & \text{if } \sigma_{n,m}(Up)>\sigma_{n,m}(Lo) \text{ and } dif_v\ge\Delta.\\ \zeta_{n,m}(i)-\dfrac{dif_v+\Delta}{2}, & \text{if } \sigma_{n,m}(Up)>\sigma_{n,m}(Lo) \text{ and } dif_v<\Delta.\end{cases} \quad (7)$$

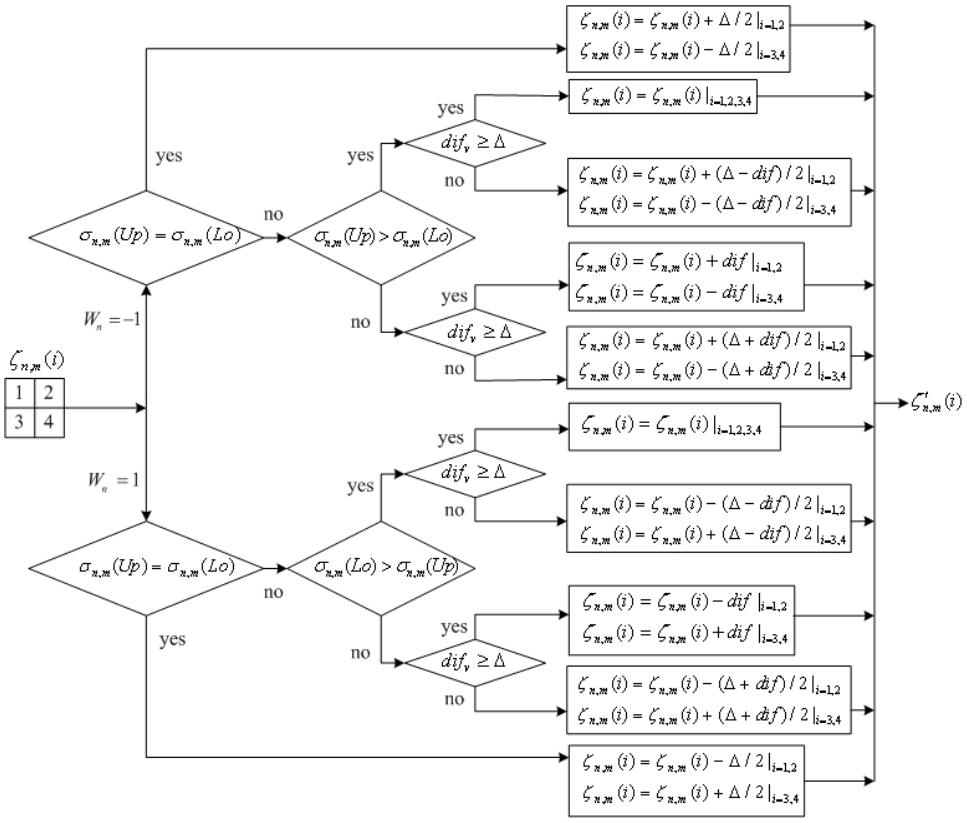

Fig. 5. The flowchart of the proposed structure-based quantization in vertical direction.

$$Q[\zeta_{n,m}(i)]|_{W_n=1}^{i=3,4} = \begin{cases} \zeta_{n,m}(i) + \dfrac{\Delta}{2}, & \text{if } \sigma_{n,m}(Up) = \sigma_{n,m}(Lo). \\ \zeta_{n,m}(i), & \text{if } \sigma_{n,m}(Lo) > \sigma_{n,m}(Up) \text{ and } dif_v \geq \Delta. \\ \zeta_{n,m}(i) + \dfrac{\Delta - dif_v}{2}, & \text{if } \sigma_{n,m}(Lo) > \sigma_{n,m}(Up) \text{ and } dif_v < \Delta. \\ \zeta_{n,m}(i) + dif_v, & \text{if } \sigma_{n,m}(Up) > \sigma_{n,m}(Lo) \text{ and } dif_v \geq \Delta. \\ \zeta_{n,m}(i) + \dfrac{dif_v + \Delta}{2}, & \text{if } \sigma_{n,m}(Up) > \sigma_{n,m}(Lo) \text{ and } dif_v < \Delta. \end{cases} \quad (8)$$

where Δ is the selected quantization step size, and dif_v is the difference in vertical direction as follows

$$dif_v = |\sigma_{n,m}(Up) - \sigma_{n,m}(Lo)| \quad (9)$$

when embedding bit W_n is "– 1", there are five cases of quantization to satisfy Eq. (4a). First, if $\sigma_{n,m}(Up) = \sigma_{n,m}(Lo)$, $\sigma_{n,m}(Up)$ and $\sigma_{n,m}(Lo)$ will be increased and decreased respectively until $dif_v = \Delta$. In case two, if $\sigma_{n,m}(Up) > \sigma_{n,m}(Lo)$ and $dif_v \geq \Delta$, $\zeta_{n,m}(i)$ will not be

modified. It is the ideal case to retain the quality. In case three, if $\sigma_{n,m}(Up) > \sigma_{n,m}(Lo)$ and $dif_v < \Delta$, $\zeta_{n,m}(i)$ will be modified to satisfy $dif_v = \Delta$. In case four, if $\sigma_{n,m}(Lo) > \sigma_{n,m}(Up)$ and $dif_v \geq \Delta$, $\sigma_{n,m}(Up)$ and $\sigma_{n,m}(Lo)$ will be increased and decreased respectively. It is the worst cast of quantization and results in large distortion. Finally, in case five, it is similar to case four, but $dif_v < \Delta$. $\sigma_{n,m}(Up)$ will be increased, and $\sigma_{n,m}(Lo)$ will be decreased until $dif_v = \Delta$. When embedding bit W_n is "1", the process of quantization is similar to embed "– 1". However, it needs to satisfy Eq. (4b). Since $\zeta_{n,m}(i)$ should be always positive or zero, the result of quantization $\zeta'_{n,m}(i)$ in Fig. 5 has a minimal value '0'.

Based on Fig. 5, we extend the subblock-wise quantization method to a super-tree quantization in Fig. 6. To quantize a super-tree is to quantize all subblocks in the super-tree. Because the elements of subblock-wise quantization should be positive, the sign bits of coefficients in the super-trees should be ignored at the quantization step. After quantization, the sign bits of coefficients will be recovered. Finally, the quantization of super-trees will result in $\zeta'_{n,m}(i)$ as follows

$$\zeta'_{n,m}(i) = Q[\zeta_{n,m}(i)],\ m = 1, \ldots, 5;\ i = 1, \ldots, 4. \tag{10}$$

Then, the super-trees $\zeta'_{n,m}(i)$ are passed through the inverse random mapping process as $\hat{f}(.)$ which recovers the original sequence of super-trees.

$$\zeta'_{k,m}(i) = \hat{f}(\zeta'_{n,m}(i)), 1 \leq n \leq 3072; 1 \leq k \leq 3072 \tag{11}$$

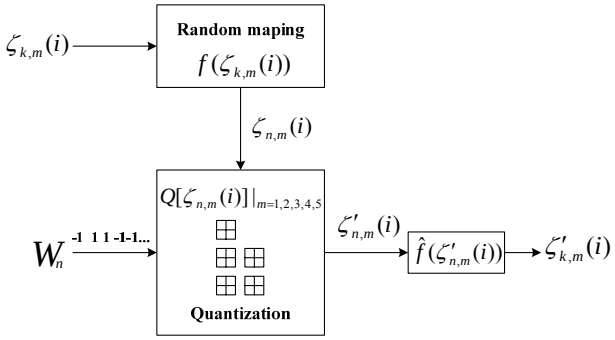

Fig. 6. Block diagram of the proposed structure-based watermark encoder.

2.4 Watermark Extraction Method

In this subsection, the watermark extraction method is described. We consider a 2 × 2 subblock $\zeta'_{n,m}$ in Eq. (11) which has been quantized. According to the proposed embedding method, there are two states of the subblock. One is $\sigma'_{n,m}(Up) > \sigma'_{n,m}(Lo)$, and the other is $\sigma'_{n,m}(Up) < \sigma'_{n,m}(Lo)$. However, if the watermarked image is attacked by distortion, the structure might be broken. It may result in the condition that $\sigma'_{n,m}(Up) = \sigma'_{n,m}(Lo)$. Hence, the bit state detector is designed by

$$D[\zeta'_{n,m}] = \begin{cases} -1, & \text{if } \sigma'_{n,m}(Up) > \sigma'_{n,m}(Lo). \\ 1, & \text{if } \sigma'_{n,m}(Up) < \sigma'_{n,m}(Lo). \\ 0, & \text{if } \sigma'_{n,m}(Up) = \sigma'_{n,m}(Lo). \end{cases} \tag{12}$$

where the case $D[\zeta'_{n,m}] = 0$ refers to the unknown state which will be used later. Similarly, the subblock-wise detector could be used as the super-tree detection. That is, to extract the bit state of a super-tree is to detect the states of all subblocks in the super-tree. Since a super-tree is composed of five 2×2 subblocks in Fig. 3, there are five extraction results. Based on these five results, we decide the final state of the super-tree by the following equation

$$S_n = \sum_{m=1}^{5} D[\zeta'_{n,m}] \tag{13}$$

where S_n is the sum of five results from Eq. (12).

Since the subblocks are located in different levels, they have different properties. Generally, the coefficients in low frequency are more stable than those in high frequency. This is because most energy usually concentrates in low frequency. To verify it, Fig. 7 shows the absolute errors of the average of subblocks in the given super-tree $\zeta_{k,m}$ upon JPEG compression with different quality factors. We can see that the average of subblocks in level three is more stable than the average in level two. It means that the subblocks in higher level have higher reliability. This property could be used in the watermark extraction method to enhance the accuracy of the detector. Hence, we proposed a novel detector. In the proposed detector, the results of the subblocks must be multiplied with the weighting factor θ_m for $m = 1, \ldots, 5$. The bigger weight refers the higher credibility, and the smaller weight refers the lower credibility of the subblocks. These weighting factors are shown as follows

$$\theta_m = \begin{cases} 3, & m = 1. \\ 1, & m = 2, 3, 4, 5. \end{cases} \tag{14}$$

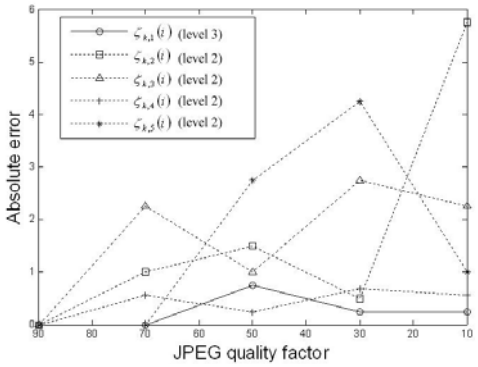

Fig. 7. The stability of the subblocks at different levels in a super-tree.

The weights are decided by two parts. One is from the subblocks in level 2, and the other is from level 3. As far as level 2 is concerned, the coefficients in the same level will have the same property of stability. Therefore, we assign the value of 1 for θ_m, $m = 2, 3, 4, 5$. For the consideration of level 3, it contains lower frequency than level 2. Hence, the coefficients in level 3 are more stable than level 2 relatively. Therefore, we should assign

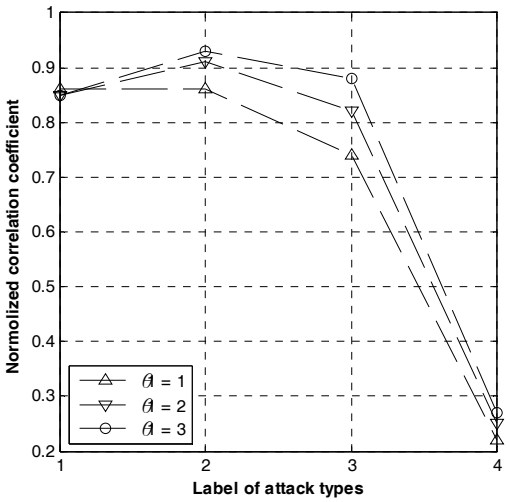

Fig. 8. The variation of Φ under different θ_1. The attack types labeled from left to right are conventional filtering, JPEG compression, median filtering and rotation.

a bigger value for θ_1. To decide this value, we do some experiments by changing the value of θ_1 as shown in Fig. 8. When θ_1 approaches 3, we can find that the correlation coefficient Φ is the maximum under all kinds of attacks except the pixel shift. For the global optimization, we finally determine $\theta_1 = 3$. Then Eq. (13) is rewritten by

$$s_n = \sum_m D[\zeta'_{n,m}] \times \theta_m. \tag{15}$$

Then, S_n is compared with a threshold $\gamma = 0$. The final state of the given super-tree is decided by

$$W'_n = \begin{cases} -1, & S_n \geq \gamma. \\ 1, & S_n < \gamma. \end{cases} \tag{16}$$

where W'_n is the extracted watermark sequence. Based on these weighting factors, the watermark will be extracted reliably. However, the extracted watermark W' from an attacked watermarked image might contain some error information. To solve this issue, the extracted watermark W' should be verified by the following equation

$$\Phi(W, W') = \frac{\sum_{n=1}^{L} W_n W'_n}{\sqrt{\sum_{n=1}^{L} W_n^2 \sum_{n=1}^{L} W_n'^2}} \tag{17}$$

where Φ is the normalized correlation coefficient which is introduced in [17, 23, 24]. It is bounded between 1 and − 1. L is the length of the watermark bit stream. To determine whether the watermark exists, a threshold Φ_T is chosen. If $\Phi \geq \Phi_T$, we say the watermark

exists. If $\Phi < \Phi_T$, the watermark does not exist. The correlation threshold Φ_T is chosen as 0.23 so that the false positive probability can be 1.03×10^{-7} which is discussed in [17].

3. ADAPTIVE STRUCTURE-BASED WATERMARKING

In this section, we will propose an adaptive quantization method to enhance the PSNR value of previous structured-based watermarking. The previous structure-based quantization mainly processes the structure in vertical direction. However, the structure in horizontal direction should be also considered. In this case, we calculate the average of the "left" two elements ($\zeta_{n,m}(1)$, $\zeta_{n,m}(3)$) and the average of the "right" two elements ($\zeta_{n,m}(2)$, $\zeta_{n,m}(4)$) in Fig. 4 as follows

$$\begin{aligned} \sigma_{n,m}(Le) &= \frac{\zeta_{n,m}(1)+\zeta_{n,m}(3)}{2}, \\ \sigma_{n,m}(Ri) &= \frac{\zeta_{n,m}(2)+\zeta_{n,m}(4)}{2}. \end{aligned} \tag{18}$$

If we embed a bit W_n in horizontal direction, $\sigma_{n,m}(Le)$ and $\sigma_{n,m}(Ri)$ will be quantized into a significant structure as $\sigma'_{n,m}(Le)$ and $\sigma'_{n,m}(Ri)$ which are given by the following equations

$$\sigma'_{n,m}(Le) > \sigma'_{n,m}(Ri), \text{ if } W_n = -1, \tag{19a}$$

$$\sigma'_{n,m}(Le) < \sigma'_{n,m}(Ri), \text{ if } W_n = 1, \tag{19b}$$

where $\sigma'_{n,m}(Le)$ and $\sigma'_{n,m}(Ri)$ are the result of quantization.

Based on this concept, an adaptive structure-based quantization in vertical or horizontal direction is proposed. We can choose two structures to quantize a given subblock $\zeta_{n,m}(i)$ in Fig. 4 as follows

$$\sigma'_{n,m}(Up) > \sigma'_{n,m}(Lo) \text{ or } \sigma'_{n,m}(Le) > \sigma'_{n,m}(Ri), \text{ if } W_n = -1, \tag{20a}$$

$$\sigma'_{n,m}(Up) < \sigma'_{n,m}(Lo) \text{ or } \sigma'_{n,m}(Le) < \sigma'_{n,m}(Ri), \text{ if } W_n = 1, \tag{20b}$$

where $\sigma'_{n,m}(Up)$, $\sigma'_{n,m}(Lo)$, $\sigma'_{n,m}(Le)$ and $\sigma'_{n,m}(Ri)$ are the results of quantization. If the embedding bit W_n is "– 1", the subblock will be quantized into a structure to satisfy $\sigma'_{n,m}(Up) > \sigma'_{n,m}(Lo)$ or $\sigma'_{n,m}(Le) > \sigma'_{n,m}(Ri)$. If the embedding bit W_n is "1", the subblock will be quantized into a structure to satisfy $\sigma'_{n,m}(Up) < \sigma'_{n,m}(Lo)$ or $\sigma'_{n,m}(Le) < \sigma'_{n,m}(Ri)$.

3.1 Adaptive Watermark Embedding Method

To satisfy Eq. (21), we proposed an adaptive structure-based wavelet-tree quantization. It can obviously enhance the PSNR value of watermarking. For example, the decision flow of structure selection for embedding bit W_n "– 1" is shown in Fig. 9. We embed the bit in the direction which results in less distortion (higher PSNR). If both directions have similar distortion, the vertical direction has higher priority than horizontal direction. Since each subblock is adaptively quantized according to the amount of distortion, this

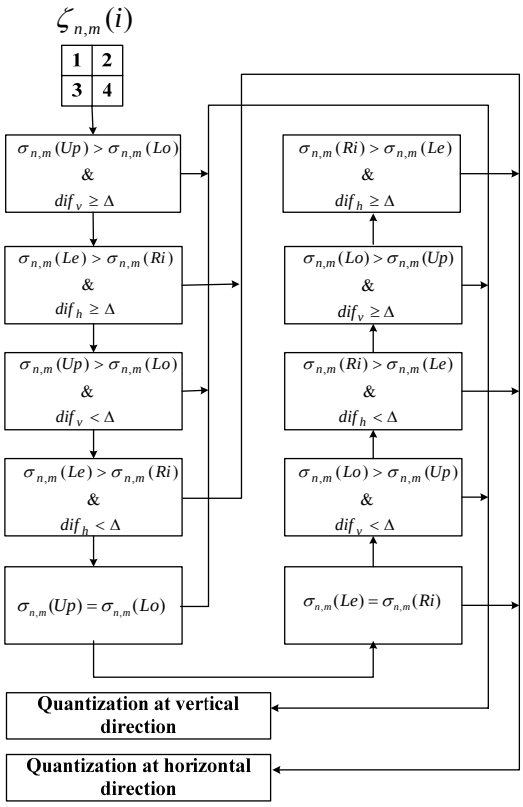

Fig. 9. Decision flow of structure selection for embedding bit W_n "– 1".

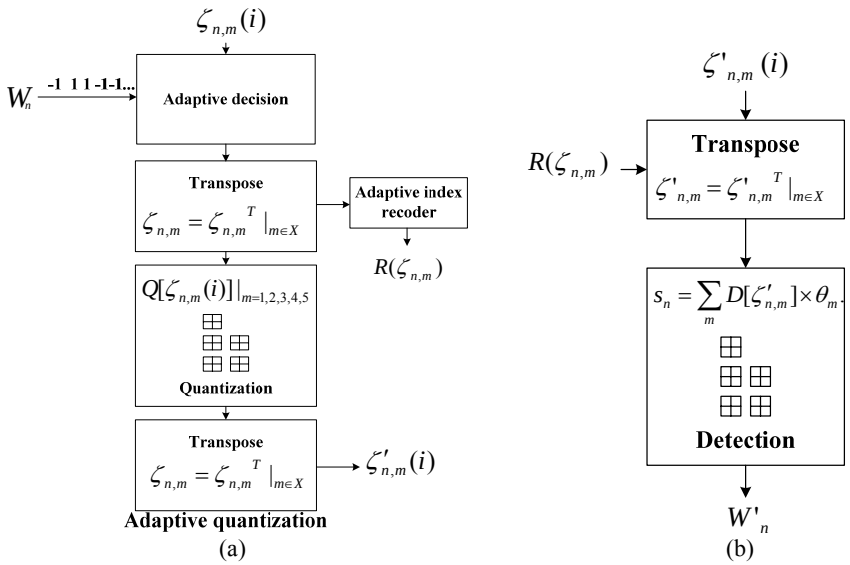

Fig. 10. (a) Proposed adaptive quantization flow; (b) Proposed adaptive watermark detection flow.

adaptive method preserves original information more precise than the previous non-adaptive structured-based watermarking. The structure/direction selection in Fig. 9 is the core of our proposed adaptive method. In this figure, dif_v denotes the difference in vertical direction, and dif_h denotes the difference in the horizontal direction as follows

$$\begin{cases} dif_v = \left|\sigma_{n,m}(Up) - \sigma_{n,m}(Lo)\right| \\ dif_h = \left|\sigma_{n,m}(Le) - \sigma_{n,m}(Ri)\right| \end{cases}. \tag{21}$$

Based on Fig. 9, we extend the above subblock quantization to a super-tree quantization in Fig. 10 (a). To quantize a super-tree is to quantize all subblocks in the super-tree. Let X be the set that the subblocks are quantized in horizontal direction. Before applying our proposed adaptive quantization flow, we use the "adaptive index recorder" in Fig. 10 (a) to save the directional information of each super-tree. There are totally 32 statuses in the adaptive quantization process, $0 \le R(\zeta_{n,m}) \le 31$. For example, when all subblocks $\zeta_{n,m}$ are quantized in "vertical" direction, we set $R(\zeta_{n,m}) = 0$. However, when all subblocks $\zeta_{n,m}$ are quantized in "horizontal" direction, we set $R(\zeta_{n,m}) = 31$. Based on $R(\zeta_{n,m})$, if the subblock does not belong to X, the quantization will use the process of Eqs. (5)-(8) in vertical direction. However, if the subblock belongs to X set, it will be quantized in horizontal direction. In this horizontal case, it will be transported and then quantized in vertical direction. After quantization, the subblock in X set will be transposed again to restore the original direction.

3.2 Adaptive Watermark Extraction Method

The adaptive extraction method is similar to the previous extraction method. The main difference between them is the additional direction information $R(\zeta_{n,m})$. For brevity, we use Fig. 10 (b) to describe the adaptive extraction flow. Firstly, the subblocks of the super-tree should be transported according to $R(\zeta_{n,m})$. Then, the super-tree will be processed by the watermark detector as Eqs. (12)-(17).

4. EXPERIMENTS

In this section, the performance of the proposed structure-based watermarking method will be tested. The quality of the watermarked images are evaluated by peak signal-to-noise ratio (PSNR), which is defined as

$$PSNR = 10 \cdot \log_{10} \frac{255^2}{MSE}, \tag{22}$$

where MSE is mean-square error. The quality of the watermarked images depends on the quantization step size Δ. Fig. 11 shows the relationship between Δ and PSNR. Based on this figure, we can find that small step size results in big PSNR, and big step size results in small PSNR. Since $\Delta = 5$ is too small to maintain robustness, we choose $\Delta = 10$ to balance the quality and robustness.

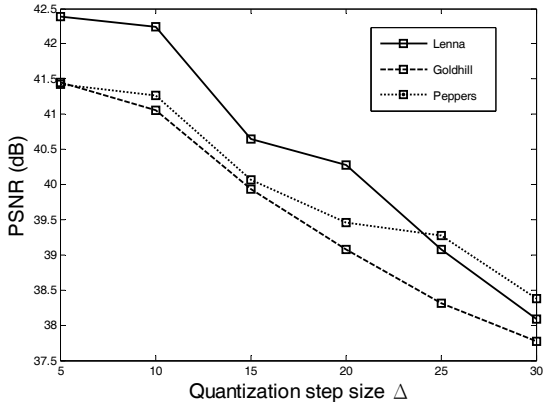

Fig. 11. PSNR of watermarked images with different quantization step size Δ.

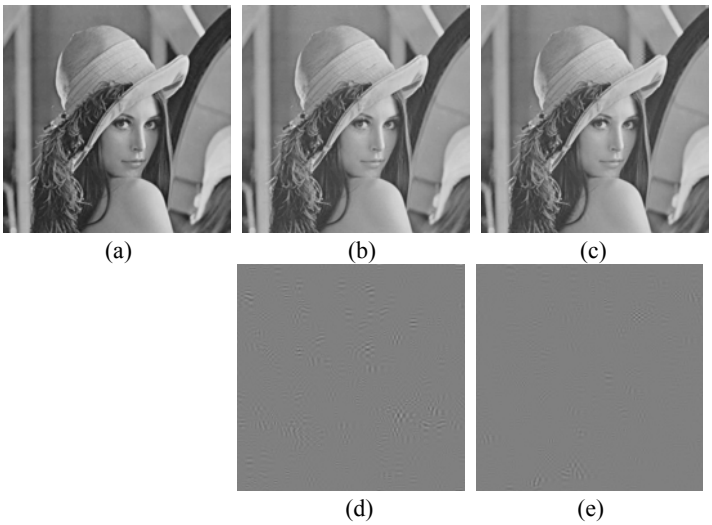

Fig. 12. (a) Original image; (b) Watermarked image with PSNR = 42.24; (c) Watermarked image with the proposed adaptive method (PSNR = 45.43); (d) Error image obtained by calculate the difference between the watermarked image and the original image; (e) Error image corresponds to the adaptive watermarked image.

Based on our proposed method, the watermark is embedded into three 512 × 512 images (Lenna, Goldhill and Peppers). The length of the watermark sequence W_n is 512. The PSNR of the proposed non-adaptive method are 42.24, 41.06 and 41.26 respectively. The PSNR of the proposed adaptive method are 45.43, 44.59 and 44.17 respectively. For brevity, only Lenna is shown. The original image of Lenna is shown in Fig. 12 (a). The watermarked image and the corresponding error image of non-adaptive method are shown in Figs. 12 (b) and (d). The watermarked image and the corresponding error image of adaptive method are shown in Figs. 12 (c) and (e). However, the method proposed by Wang *et al*. [17] only has 38.2, 38.7 and 39.8 respectively. Compared with Wang *et al*., the proposed non-adaptive method improves PSNR about 2.62 dB and the proposed adaptive

method greatly increases PSNR about 5.83 dB. The total capacity for embedding is also increased about 2304. In addition, we must also verify whether the proposed method is robust for watermarking. Hence, we do some experiments in order to test the robustness. Several kinds of attacks will be applied to the watermarked image.

Generally, the common attacks are classified into nongeometric and geometric methods. The nongeometric attack includes filtering like median filter, Gaussian filter and sharpening or image compression like JPEG. The geometric attack includes pixel shifting. Based on these attacks, the corresponding results are given next.

JPEG compression: In Table 1, the watermarked image is suffered by JPEG compression. Lower quality factor value means higher compression ratio. Quality factors of 10, 30, 50, 70 and 90 are used to test the existence of watermark. In addition, this table also shows the normalized correlation coefficient Φ. Compared with Wang *et al*. [17], our proposed method can resist higher compression ratio attack.

Filter: The watermarked image is suffered by median filter in Table 2. Median filter with radius 2 and 3 are selected to attack the watermarked image. Since the proposed method

Table 1. Correlation coefficient Φ and watermark existence upon JPEG compression with quality factor 30, 50, 70, 90.

(a) LENNA.

JPEG	Proposed method (non-adaptive)		Proposed method (adaptive)		Wang's method	
	Φ	Existence	Φ	Existence	Φ	Existence
90	1	Y	1	Y	1	Y
70	1	Y	1	Y	0.57	Y
50	0.99	Y	0.99	Y	0.26	Y
30	0.93	Y	0.91	Y	0.15	N
average	0.98		0.98		0.5	

(b) GOLDHILL.

JPEG	Proposed method (non-adaptive)		Proposed method (adaptive)		Wang's method	
	Φ	Existence	Φ	Existence	Φ	Existence
90	1	Y	1	Y	1	Y
70	1	Y	1	Y	0.93	Y
50	1	Y	1	Y	0.71	Y
30	0.97	Y	0.94	Y	0.23	Y
average	0.99		0.99		0.72	

(c) PEPPERS.

JPEG	Proposed method (non-adaptive)		Proposed method (adaptive)		Wang's method	
	Φ	Existence	Φ	Existence	Φ	Existence
90	1	Y	1	Y	1	Y
70	1	Y	1	Y	0.97	Y
50	1	Y	0.99	Y	0.70	Y
30	0.94	Y	0.92	Y	0.34	Y
average	0.99		0.98		0.75	

Table 2. Correlation coefficient Φ and watermark existence upon attack of median filter with radius 2, 3.

(a) LENNA.

Median filter	Proposed method (non-adaptive)		Proposed method (adaptive)		Wang's method	
	Φ	Existence	Φ	Existence	Φ	Existence
2	0.79	Y	0.84	Y	0.38	Y
3	0.46	Y	0.62	Y	0.51	Y
average	0.63		0.73		0.45	

(b) GOLDHILL.

Median filter	Proposed method (non-adaptive)		Proposed method (adaptive)		Wang's method	
	Φ	Existence	Φ	Existence	Φ	Existence
2	0.67	Y	0.73	Y	0.35	Y
3	0.30	Y	0.42	Y	0.56	Y
average	0.49		0.58		0.46	

(c) PEPPERS.

Median filter	Proposed method (non-adaptive)		Proposed method (adaptive)		Wang's method	
	Φ	Existence	Φ	Existence	Φ	Existence
2	0.81	Y	0.88	Y	0.46	Y
3	0.45	Y	0.59	Y	0.71	Y
average	0.63		0.74		0.59	

Table 3. Correlation coefficient Φ and watermark existence upon attack of Gaussian filter.

(a) LENNA.

Gaussian filter	Proposed method (non-adaptive)		Proposed method (adaptive)		Wang's method	
	Φ	Existence	Φ	Existence	Φ	Existence
	0.82	Y	0.82	Y	0.64	Y

(b) GOLDHILL.

Gaussian filter	Proposed method (non-adaptive)		Proposed method (adaptive)		Wang's method	
	Φ	Existence	Φ	Existence	Φ	Existence
	0.63	Y	0.75	Y	0.56	Y

(c) PEPPERS.

Gaussian filter	Proposed method (non-adaptive)		Proposed method (adaptive)		Wang's method	
	Φ	Existence	Φ	Existence	Φ	Existence
	0.70	Y	0.78	Y	0.74	Y

gains bigger average value of Φ, it outperforms Wang's method. In Table 3, the watermarked image is suffered by Gaussian filter [25]. Since the proposed method gains bigger value of Φ than Wang's method, the proposed method is more robust than Wang's method.

Sharpening: In Table 4, the watermarked image is applied by sharpening. Result shows that the proposed method performs very well. It has strong robustness in this topic.

Geometric attacks: The common watermarking methods are usually location based technique. Since the geometric attacks change the location of pixels, these attacks sometimes

Table 4. Correlation coefficient Φ and watermark existence upon sharpening.

(a) LENNA.

Sharpening	Proposed method (non-adaptive)		Proposed method (adaptive)		Wang's method	
	Φ	Existence	Φ	Existence	Φ	Existence
	1	Y	1	Y	0.46	Y

(b) GOLDHILL.

Sharpening	Proposed method (non-adaptive)		Proposed method (adaptive)		Wang's method	
	Φ	Existence	Φ	Existence	Φ	Existence
	1	Y	1	Y	0.39	Y

(c) PEPPERS.

Sharpening	Proposed method (non-adaptive)		Proposed method (adaptive)		Wang's method	
	Φ	Existence	Φ	Existence	Φ	Existence
	0.99	Y	1	Y	0.62	Y

Table 5. Correlation coefficient Φ and watermark existence upon attack of circular pixel shift with 5-10 pixels.

(a) LENNA.

Pixel shift	Proposed method (non-adaptive)		Proposed method (adaptive)		Wang's method	
	Φ	Existence	Φ	Existence	Φ	Existence
5	0.55	Y	0.49	Y	0.28	Y
7	0.39	Y	0.35	Y	0.29	Y
9	0.59	Y	0.48	Y	0.26	Y
10	0.33	Y	0.32	Y	0.19	N
average	0.47		0.41		0.26	

(b) GOLDHILL.

Pixel shift	Proposed method (non-adaptive)		Proposed method (adaptive)		Wang's method	
	Φ	Existence	Φ	Existence	Φ	Existence
5	0.46	Y	0.36	Y	0.36	Y
7	0.46	Y	0.34	Y	0.41	Y
9	0.56	Y	0.32	Y	0.29	Y
10	0.32	Y	0.23	Y	0.21	N
average	0.45		0.31		0.32	

(c) PEPPERS.

Pixel shift	Proposed method (non-adaptive)		Proposed method (adaptive)		Wang's method	
	Φ	Existence	Φ	Existence	Φ	Existence
5	0.57	Y	0.45	Y	0.32	Y
7	0.39	Y	0.27	Y	0.29	Y
9	0.46	Y	0.32	Y	0.29	Y
10	0.24	Y	0.25	Y	0.26	Y
average	0.42		0.32		0.29	

make the watermark extraction fail. Hence, the robustness for geometric attacks is an important issue in recent research of watermarking. In Table 5, it is the circular pixel shifting attack which moves the pixels of the watermarked image in horizontal direction. If the pixels are moved outside the boundary of image, they will be moved to the opposite

Table 6. Correlation coefficient Φ and watermark existence upon attack of line deletion pixel shift with 5-10 pixels.

(a) LENNA.

Pixel shift	Proposed method (non-adaptive)		Proposed method (adaptive)		Wang's method	
	Φ	Existence	Φ	Existence	Φ	Existence
5	0.49	Y	0.38	Y	0.27	Y
7	0.41	Y	0.25	Y	0.27	Y
9	0.53	Y	0.41	Y	0.25	Y
10	0.29	Y	0.23	Y	0.17	N
average	0.43		0.32		0.24	

(b) GOLDHILL.

Pixel shift	Proposed method (non-adaptive)		Proposed method (adaptive)		Wang's method	
	Φ	Existence	Φ	Existence	Φ	Existence
5	0.5	Y	0.38	Y	0.37	Y
7	0.41	Y	0.36	Y	0.43	Y
9	0.47	Y	0.31	Y	0.25	Y
10	0.3	Y	0.19	N	0.20	N
average	0.42		0.31		0.31	

(c) PEPPERS.

Pixel shift	Proposed method (non-adaptive)		Proposed method (adaptive)		Wang's method	
	Φ	Existence	Φ	Existence	Φ	Existence
5	0.54	Y	0.48	Y	0.34	Y
7	0.41	Y	0.34	Y	0.31	Y
9	0.42	Y	0.34	Y	0.28	Y
10	0.23	Y	0.23	Y	0.27	Y
average	0.4		0.35		0.3	

side. In Table 6, it is the line deletion pixel shifting attack. Tables 5 and 6 show that the proposed method gains higher robustness in this topic.

In Table 7, rotation attack with degree from – 1 to 1 are applied into watermarked images. The normalized correlation coefficient of proposed method is bigger than the method proposed by Wang *et al.* [17] under the degree 0.25 and 0.5. Hence, our proposed method is very robust under this condition. Out of this range, Wang *et al.* [17] is better than ours. No matter what geometrical attack is, the PSNR of our proposed method is always higher than Wang's method. Since the geometrical attacks are much different to the conventional filtering attacks, we will make further research on this topic in the future.

Multiple watermark attack: If one attacker wants to confuse the detector or destroy the watermarked image, he may apply the same quantization method many times for multiple watermark attack. Although attacker may know the method of watermarking, he does not have the key of the random mapping function in Eq. (2). Table 8 shows the robustness of the multiple watermark attack. The experimental result shows that the proposed method is very robust to against the multiple watermark attack. When the number of watermarks is "4" which makes Wang's method fail to work, our proposed method still works well in this condition. In addition, the average PSNR is higher than Wang's method.

Table 7. Correlation coefficient Φ and watermark existence upon attack of rotation and scaling.

(a) LENNA.

Rotation	Proposed method (non-adaptive)		Proposed method (adaptive)		Wang's method	
	Φ	Existence	Φ	Existence	Φ	Existence
0.25	0.7	Y	0.8	Y	0.37	Y
0.5	0.24	Y	0.38	Y	0.29	Y
0.75	0.16	N	0.21	N	0.26	Y
1	0	N	0.13	N	0.24	Y
average	0.28		0.38		0.29	

(b) GOLDHILL.

Rotation	Proposed method (non-adaptive)		Proposed method (adaptive)		Wang's method	
	Φ	Existence	Φ	Existence	Φ	Existence
0.25	0.57	Y	0.63	Y	0.33	Y
0.5	0.24	Y	0.25	Y	0.24	Y
0.75	0.1	N	0.16	N	0.21	N
1	0.02	N	0.05	N	0.15	N
average	0.23		0.27		0.23	

(c) PEPPERS.

rotation	Proposed method (non-adaptive)		Proposed method (adaptive)		Wang's method	
	Φ	Existence	Φ	Existence	Φ	Existence
0.25	0.57	Y	0.66	Y	0.41	Y
0.5	0.3	Y	0.32	Y	0.3	Y
0.75	0.07	N	0.2	N	0.26	Y
1	0.1	N	0.1	N	0.17	N
average	0.26		0.32		0.29	

Table 8. Correlation coefficient Φ and watermark existence upon attack of multiple watermark.

(a) LENNA.

Number of watermarks	Proposed method (non-adaptive)			Proposed method (adaptive)			Wang's method		
	PSNR	Φ	Existence	PSNR	Φ	Existence	PSNR	Φ	Existence
1	41.72	0.84	Y	44.86	0.96	Y	35.50	0.65	Y
2	41.67	0.67	Y	44.53	0.93	Y	32.78	0.41	Y
3	41.81	0.58	Y	44.37	0.91	Y	29.35	0.27	Y
4	41.53	0.46	Y	44.21	0.86	Y	28.05	0.11	N
average	41.68	0.64		44.49	0.92		31.42	0.36	

(b) GOLDHILL.

Number of watermarks	Proposed method (non-adaptive)			Proposed method (adaptive)			Wang's method		
	PSNR	Φ	Existence	PSNR	Φ	Existence	PSNR	Φ	Existence
1	40.14	0.88	Y	43.99	0.95	Y	35.26	0.79	Y
2	40.09	0.75	Y	43.45	0.91	Y	31.50	0.45	Y
3	40.06	0.59	Y	43.52	0.86	Y	29.71	0.31	Y
4	39.57	0.50	Y	43.78	0.83	Y	28.57	0.18	N
average	39.97	0.68		43.67	0.9		31.26	0.43	

Table 8. (Cont'd) Correlation coefficient Φ and watermark existence upon attack of multiple watermark.

(c) PEPPERS.

Number of watermarks	Proposed method (non-adaptive)			Proposed method (adaptive)			Wang's method		
	PSNR	Φ	Existence	PSNR	Φ	Existence	PSNR	Φ	Existence
1	40.98	0.83	Y	43.88	0.95	Y	34.53	0.80	Y
2	40.76	0.68	Y	43.56	0.86	Y	31.99	0.53	Y
3	40.60	0.58	Y	43.20	0.81	Y	30.19	0.31	Y
4	39.76	0.47	Y	42.46	0.78	Y	28.81	0.22	N
average	40.53	0.64		43.32	0.85		31.38	0.47	

Table 9. The experimental parameters of the proposed method and Wang *et al.* [17].

Parameters	Proposed method	Wang's method [17]
DWT decomposition level	3	4
Number of coefficients in a super-tree	20	42
Number of super-trees for embedding a bit	1	1
Capacity (bits)	3072	768
Host image size	512	512
Watermark length	512	512

To show the fairness of the comparison with Wang-Lin's method, the parameters of the both methods are shown in Table 9. The testing host images for both methods are the same ones with the same size. In this table, we show the experimental parameters of the proposed method and Wang's method. In Wang's method, the number of coefficients for embedding a bit reaches 42. However, we only need 20 which is half number of Wang's method. Intuitively, small number of coefficients for embedding a bit may decrease the robustness. Although our proposed method has made a concession in the performance comparison, it still reaches good performance. Besides, we also increase the capacity for embedding watermark to be 3072. It's 4 times as great as Wang's method. For the consideration of DWT decomposition, Wang's method needs 4-level. Compared with Wang's method, we only need 3-level. It means we need less computation than Wang's method.

The proposed adaptive structure-based watermarking has the advantages in robustness and quality. Furthermore, we should analyze the computation load. The CPU time of all algorithms running in Pentium IV 3.2GHz are compared as follows:

- Watermark embedding process:
  - Proposed structure-based watermarking method (1.60 s).
  - Proposed adaptive structure-based watermarking method (1.66 s).
  - Wang's method (12.4 s).

- Watermark extraction process:
  - Proposed structure-based watermarking method (0.73 s).
  - Proposed adaptive structure-based watermarking method (0.75 s).
  - Wang's method (10.78 s).

Since Wang's method needs to spread each pair of super-trees into bitplane, the related quantization process results in much computation load. Hence, the above experimental results show that our proposed adaptive structure-based method has the advantage of low computation load.

5. CONCLUSIONS

This work presents a structure-based wavelet-tree quantization method for image copyright protection. This structure-based watermarking method adopts the coefficient correlation of the subblocks in super-trees. The proposed structure-based quantization method quantizes the super-trees into a significant structure. The quantized structure has a stronger statistical characteristic than an unquantized super-tree structure. This characteristic enables the watermark bits to be extracted robustly after an image distortion attack. Experimental results demonstrate that the proposed method achieves a high image quality (PSNR) and strong robustness. To further enhance the PSNR value of the proposed structure-based method, an adaptive structure-based watermarking is presented. Compared with the proposed non-adaptive method, it increases PSNR about 3.21 dB. Compared with Wang's method, it greatly increases PSNR about 5.83 dB. The adaptive method also has a high maximum number of watermark bits, giving it a high embedding capacity. Moreover, the computation load of the proposed method is small. Experimental results demonstrate that the proposed watermarking using adaptive structure-based wavelet-tree quantization performs well in JPEG compression, filtering (Gaussian filter, median filter and sharpen) and geometric attacks (pixel shifting and rotation). Besides, it is also very robust to multiple watermark attacks.

REFERENCES

1. J. Meng and S. F. Chang, "Embedding visible video watermarks in the compressed domain," in *Proceedings of the International Conference on Image Processing*, Vol. 1, 1998, pp. 474-477.
2. M. S. Kankanhalli, Rajmohan, and K. R. Ramakrishnan, "Adaptive visible watermarking of images," in *Proceedings of the International Conference on Multimedia Computing and Systems*, Vol. 1, 1999, pp. 568-573.
3. P. M. Chen, "A visible watermarking mechanism using a statistic approach," in *Proceedings of the International Conference on Signal Processing*, Vol. 2, 2000, pp. 910-913.
4. R. G. Schyndel, A. Z. Tirkel, and C. F. Osborne, "A digital watermark," in *Proceedings of the International Conference on Image Processing*, Vol. 2, 1994, pp. 86-90.
5. A. Nikolaidis and I. Pitas, "Region-based image watermarking," *IEEE Transactions on Image Processing*, Vol. 10, 2001, pp. 1726-1740.
6. C. S. Lu and H. Y. M. Liao, "Structural digital signature for image authentication: an incidental distortion resistant scheme," *IEEE Transactions on Multimedia*, Vol. 5, 2003, pp. 161-173.
7. G. C. Langelaar and R. L. Langendijk, "Optimal differential energy watermarking of DCT encoded images and video," *IEEE Transactions on Image Processing*, Vol. 10,

2001, pp. 148-158.
8. X. Li and X. Xue, "A novel blind watermarking based on lattice vector quantization," in *Proceedings of the International Conference on Electrical and Computer Engineering*, Vol. 3, 2004, pp. 1823-1826.
9. J. R. Hernandez, M. Amado, and F. Perez-Gonzalez, "DCT-domain watermarking techniques for still image: Detector performance analysis and a new structure," *IEEE Transactions on Image Processing*, Vol. 9, 2000, pp. 55-68.
10. Y. P. Hu and D. Z. Han, "Wavelet-based readable watermarking algorithm using adaptive quantization," in *Proceedings of the International Conference on Image Machine Learning and Cybernetics*, Vol. 7, 2004, pp. 4076-4080.
11. D. Kundur and D. Hatzinakos, "Digital watermarking, using multiresolution wavelet decomposition," in *Proceedings of the International Conference on Acoustics, Speech and Signal*, Vol. 5, 1998, pp. 2969-2972.
12. Y. H. Chen, J. M. Su, H. C. Fu, H. C. Huang, and H. T. Pao, "Adaptive watermarking using relationships between wavelet coefficients," in *Proceedings of the International Symposium on Circuits and Systems*, Vol. 5, 2005, pp. 4979-4982.
13. C. S. Lu and H. Y. Liao, "Multipurpose watermarking for image authentication and protection," *IEEE Transactions on Image Processing*, Vol. 10, 2001, pp. 1579-1592.
14. M. J. Tsai, K. Y. Yu, and Y. Z. Chen, "Joint wavelet and spatial transformation for digital watermarking," *IEEE Transactions on Consumer Electron*, Vol. 46, 2000, pp. 137-144.
15. J. M. Shapiro, "Embedded image coding using zerotrees of wavelet coefficients," *IEEE Transactions on Signal Processing*, Vol. 41, 1993, pp. 3445-3462.
16. M. S. Hsieh, D. C. Tseng, and Y. H. Huang, "Hiding digital watermarks using multiresolution wavelet transform," *IEEE Transactions on Industrial Electronics*, Vol. 48, 2001, pp. 875-882.
17. S. H. Wang and Y. P. Lin, "Wavelet tree quantization for copyright protection watermarking," *IEEE Transactions on Image Processing*, Vol. 13, 2004, pp. 154-165.
18. H. Liu, J. Lin, and J. Huang , "Image authentication using content based watermark," in *Proceedings of the International Symposium on Circuits and Systems*, Vol. 4, 2005, pp. 4014-4017.
19. K. Su, D. Kundur, and D. Hatzinakos, "Spatially localized image-dependent watermarking for statistical invisibility and collusion resistance," *IEEE Transactions on Multimedia*, Vol. 7, 2005, pp. 52-66.
20. P. Dong, J. G. Brankov, N. P. Galatsanos, Y. Yang, and F. Davoine, "Digital watermarking robust to geometric distortions," *IEEE Transactions on Image Processing*, Vol. 14, 2005, pp. 2140-2150.
21. V. Licks and R. Jordan, "Geometric attacks on image watermarking systems," *IEEE Transactions on Multimedia*, Vol. 12, 2005, pp. 68-78.
22. W. Zeng and B. Liu, "A statistical watermark detection technique without using original images for resolving rightful ownerships of digital images," *IEEE Transactions on Image Processing*, Vol. 8, 1999, pp. 1534-1548.
23. C. T. Hsu and J. L. Wu, "Hidden digital watermarks in images," *IEEE Transactions on Image Processing*, Vol. 8, 1999, pp. 58-68.
24. C. T. Hsu and J. L. Wu, "DCT-based watermarking for video," *IEEE Transactions on Consumer Electronics*, Vol. 44, 1998, pp. 206-216.

25. A. R. Weeks, Jr., *Fundamentals of Electronic Image Processing*, Wiley-IEEE Press, Bellingham, 1996.

Gin-Der Wu (吳俊德) received the B.S. degree in Engineering Science from the National Cheng Kung University, Tainan, Taiwan, R.O.C. in 1996 and the Ph.D. degree in Electrical and Control Engineering from the National Chiao Tung University, Hsinchu, Taiwan, R.O.C. in 2000. In 2002, he joined VIA Technologies, INC., as a senior engineer in Chipset R&D Division. In 2003, he joined ALI Corporation, as a senior engineer in Digital AV Product Business Division. Since February 2004, he joined the National Chi Nan University, Nantou, Taiwan, R.O.C., where he is currently an Assistant Professor of Electrical Engineering. His current research interests are digital signal processing, neural fuzzy networks, and VLSI chip design.

Pang-Hsuan Huang (黃邦瑄) received the M.S. degree in Electrical Engineering from the National Chi Nan University in 2007. He is pursuing Ph.D. in the National Chi Nan University. His current research interests include digital watermarking, speaker recognition.